Inositol 1,4,5-trisphosphate 3-kinase A overexpression induces cytoskeletal re-organization and increases migration via a kinase-independent mechanism

Sabine Windhorst, Christine Blechner, Hong-Ying Lin, Christian Elling, Marcus Nalaskowski, Tanja Kirchberger, Andreas H Guse, Georg W Mayr

Inositol 1,4,5-trisphosphate 3-kinase A overexpression induces cytoskeletal re-organization and increases migration via a kinase-independent mechanism

Sabine Windhorst, Christine Blechner, Hong-Ying Lin, Christian Elling, Marcus Nalaskowski, Tanja Kirchberger, Andreas H. Guse and Georg W. Mayr

Institut für Biochemie und Molekularbiologie I: Zelluläre Signaltransduktion, Universitätsklinikum Hamburg-Eppendorf, Martinistr. 52, D-20246 Hamburg, Germany

Address correspondence to: Sabine Windhorst, Institut für Biochemie und Molekularbiologie I: Zelluläre Signaltransduktion, Universitätsklinikum Hamburg-Eppendorf, Martinistr. 52, D-20246 Hamburg, Germany, Tel. +49-40-42803-6341; Fax: +49-40-42803-6818; E-mail: s.windhorst@uke.uni-hamburg.de

Running title Overexpression of IP3K-A increases cell migration

Keywords Cell motility, actin remodeling, branching protrusions

Biochemical Journal Immediate Publication. Published on 23 May 2008 as manuscript BJ20080630

In this study effects of increased inositol 1,4,5-trisphosphate 3-kinases-A (IP3K-A) expression were analyzed. H1299 cells overexpressing IP3K-A formed branching protrusions and under three-dimensional culture conditions they exhibited a motile fibroblast-like morphology. They lost the ability to form actin stress fibers and showed increased invasive migration in vitro. Furthermore, expression levels of the mesenchymal marker proteins vimentin and N-cadherin were increased. The enzymatic function of IP3K-A is to phosphorylate the calcium mobilizing second messenger D-*myo*-inositol 1,4,5-trisphosphate (Ins(1,4,5)P_3) to D-*myo*-inositol 1,3,4,5-tetrakisphosphate (Ins(1,3,4,5)P_4). Accordingly, cells overexpressing IP3K-A showed reduced calcium release and altered concentrations of inositol phosphates, with decreasing concentrations of Ins(1,4,5)P_3, inositol hexakisphosphate and inositol 1,2,3,4,5 pentakisphosphate, and increasing concentrations of Ins(1,3,4,5)P_4. However, IP3K-A induced effects on cell morphology do not seem to be dependent on enzyme activity since a protein devoid of enzyme activity also induced formation of branching protrusions. Therefore, we propose that the morphological changes induced by IP3K-A are mediated by non-enzymatic activities of the protein.

INTRODUCTION

Inositol 1,4,5-trisphosphate 3-kinase-A (IP3K-A) is one out of three isoforms (A, B and C) that catalyse the phosphorylation of the calcium mobilizing second messenger D-*myo*-inositol 1,4,5-trisphosphate ($Ins(1,4,5)P_3$) to D-*myo*-inositol 1,3,4,5-tetrakisphosphate ($Ins(1,3,4,5)P_4$) [1]. This IP3K product is involved in the regulation of calcium influx [2-4], and interferes with the Ras- and the phosphoinositide-3 kinase-pathway. High cellular concentrations of $Ins(1,3,4,5)P_4$ can compete for binding of Ras-GTPase activating protein (Ras-GAP) to phosphatidylinositol 4,5-bisphosphate ($PtdIns(4,5)P_2$) [5], resulting in translocation of Ras-GAP to the cytosol and in unhindered activation of Ras [6]. Additionally, it was demonstrated that, up to a certain threshold level, $Ins(1,3,4,5)P_4$ mediates promotion of pleckstrin homology domain (PH domain) binding to phosphatidylinositol 3,4,5-trisphosphate ($PtdIns(3,4,5)P_3$) [7]. In addition to its function as a potential second messenger, $Ins(1,3,4,5)P_4$ serves as substrate for the production of further higher phosphorylated inositols, which have been implicated in multiple cellular processes (for review, see [8]).

Although all IP3K isoforms catalyze the same step in inositol phosphate metabolism, their physiological functions are different. Isoforms B and C are ubiquitously expressed [9,10] and both isoforms seem to play a special role in immune cell development [11,12]. IP3K-A is a neuron and testis specific isoform [13]. There are no data available about its role in testis, but in neurons expression levels, activity and localization of IP3K-A was investigated. In theses cells IP3K-A is located in dendritic spines and shows exclusive F-actin localization [14,15]. In embryonic rat neurons its activity is low and increases until the age of four month [16], whereby the highest expression level was found in hippocampal pyramidal cells [17]. Since its expression further increases during spatial learning [18] and IP3K-A knock out in mice revealed that the kinase influences long term potentiation [19], it is assumed that the protein has rele-

vance in memory formation [18]. However, the exact physiological role of IP3K-A expression has not been elucidated yet.

In the present study we used a cell model to examine the effect of increased IP3K-A expression on proliferation, migration and cell morphology. We found that overexpression of IP3K-A in H1299 cells changed morphology through reorganization of the cytoskeleton and increased cellular migration, most likely due to non-enzymatic activity.

MATERIAL AND METHODS

Materials

H1299 cells were kindly provided by Dr. Günes (Heinrich Pette Institut, Hamburg, Germany, for characterization see American Type Culture Collection, (ATCC)). The cells were cultured in DMEM supplemented with 10% (v/v) fetal calf serum (FCS), 4 mM L-glutamine, 100 µg/ml streptomycin and 100 U/ml penicillin. Culture media and G418 were obtained from Invitrogen (Groningen, Netherlands). Extracellular Matrix gel derived from the Engelbreth-Holm-Swarm mouse sarcoma was from Sigma (München, Germany). Antibodies were from Santa Cruz (Heidelberg, Germany), and from BD Biosciences (Heidelberg, Germany). FuGENE6 and G-Sepharose were from Roche (Alameda, CA) and the pEGFP plasmid from Clontech (Saint-Germain-en-Laye, France). Fura-2/AM was purchased from Calbiochem (Darmstadt, Germany). All chemicals used were of the highest quality available.

Construction of fusion genes and fusion gene derivates

The full-length cDNA clone IMAGE:4792595 (GenBank accession no. BC026331; GenBank gi 20072242) encoding human IP3K-A was obtained from ResGen Invitrogen Corporation (Carlsbad, USA), and completely sequenced. The enhanced green fluorescent protein (EGFP) fusion gene GFP-IP3KA was created by standard PCR techniques. Because of the GC-rich 5'-end of the cDNA (>80% GC), dimethyl sulfoxide (DMSO) or tetramethylene sulfoxide (TMSO) was added to a final concentration of 10% and 5% (v/v), respectively [20]. The open reading frame was amplified using the following primer pairs: GFP-IP3KA, 5'-CAA GCT TCG ATG ACC CTG CCC GGG GGC CC-3' and 5'-AGG TAC CTC ATC TCT CAG CCA GGC TGG-3'. The PCR products were A-tailed and initially cloned into the pGEM T-Easy vector from Promega (Mannheim, Germany). The open reading frame was again completely sequenced to check PCR fidelity, and then the fragment was subcloned using the restriction sites introduced (HindIII/KpnI) into the expression vector pEGFP-C1 (Clontech).

The point mutation mut1 (D^{416}→N), the deletion mutant mut2 (aa 2-66 deleted) and mut3 (P^{67}→stop) were created by using modified QuikChange site-directed mutagenesis [21]. The GFP-IP3KA fusion gene was used as template. PCR fidelity of the constructs was checked by complete sequencing of the coding region.

Establishment of H1299 clones overexpressing IP3K-A

Transfection for stable expression of GFP-IP3KA was performed by FuGENE6 according to manufacturer's instructions. Cells were transfected with pEGFP-C1-IP3K-A or pEGFP, followed by G418-selection of lines. Clones were isolated by fluorescence activated cell sorting (using a BD FACSAria™ cell sorter) based on the GFP fluorescence and examined for the expression of GFP-IP3K-A fusion proteins by immunoblotting with anti-GFP or anti-IP3K-A antibodies.

Immunoprecipitation

50 µl protein G sepharose beads were incubated with anti-GFP antibody, anti-IP3K-A antibody, or anti-ERK1/2 antibody (volume: 12.5 µl; concentration: 200 µg/ml in PBS) over night at 4 °C. Cells, overexpressing GFP-IP3K-A or GFP, grown to 80% confluence in 15 cm dishes, were lysed with 2 ml MPER (mammalian protein-extraction reagent; Pierce) supplemented with protease inhibitor cocktail (Roche), transferred into a microtube and frozen in liquid nitrogen. After thawing and centrifugation (10 min; 13.000 g; 4 °C) the supernatant was incubated with G sepharose beads over night at 4 °C. Then, the G sepharose was washed 3 times with PBS and used for determination of IP3K-A enzyme activity or was supplied to SDS-PAGE.

Determination of IP3K-A enzyme activity by HPLC

30 µl of immunoprecipitated GFP-IP3K-A or GFP (see above) suspension was added to 270 µl reaction buffer (10 mM triethanolamine-HCl, 30 mM KCl, 1 mM DTT, 500 µM ATP, 5 mM $MgCl_2$, 7.5 nmol Ins(1,4,5)P_3; pH 7.5) and incubated at 30 °C. After 0, 10, 20, 30, and 60 min 50 µl were withdrawn and diluted in 350 µl cold water. Nucleotides were removed by extraction with charcoal and inositol phosphates were analyzed by micrometal dye detection HPLC (MDD-HPLC) [22,23] To calculate specific enzyme activity the concentration of purified GFP-IP3K-A was determined from Coomassie Blue stained SDS gels using BSA as standard.

Determination of cell proliferation

$1x10^4$ cells were seeded per well in 96 well plates and incubated at 37 °C and 5% CO_2 for 24, 48 and 72 h. Growth was determined by counting trypsinized cells, using a CASY-1 cell counter (Schärfe System, Reutlingen, Germany).

Immunoblotting and immunofluorescence

Immunofluorescence and Immunoblotting were performed as described [24].

In vitro migration assay in Boyden chambers

Boyden chambers (costar) with 3 µm pore size membrane inserts were covered with extracellular matrix (ECM) from Sigma according to manufacturer's instructions. 5000 cells per well, suspended in DMEM containing 10% FCS, were seeded in each chamber and were incubated for 16 h at 37 °C in 5% CO_2. Then the ECM was removed by a cotton swab and, after washing 3 times with PBS, cells having permeated the membrane pores were fixed with 3% paraformaldehyde. DAPI stained cells were counted using immunofluorescence microscopy.

Staining for F-actin

Cells were seeded in chamber slides, grown to 50% confluence, washed with PBS and fixed with 3% paraformaldehyd for 10 min at 37°C. After washing with PBS, the cells were incubated for 10 min with TRITC-phalloidin. Then, the cells were washed again and monitored by fluorescence microscopy.

Cultivation of H1299 cells in porous cellulose capillary

Cells were grown to about 80% confluence in a 75 cm^2 flask. After trypsinizing, they were suspended in 1 ml DMEM/10% FCS and transferred into a petri dish. The cell

suspension was aspirated into porous cellulose capillary tubes permeable to medium with an inner diameter of 200 microns and 2 cm length [25], placed in 6 well plates (four capillaries per well) and grown for 72 h in 5% CO_2 at 37 °C. Growth behavior of cells was monitored every 24 h by light microscopy.

Metal dye detection HPLC analysis of inositol phosphates (MDD-HPLC)

H1299 cells ($4x10^6$) were plated on 15 cm cell culture dishes. After 48 h, dishes were placed on ice and washed twice with ice cold PBS. After completely removing the PBS, 1 ml ice-cold trichloracetic acid (8%) supplemented with 10 µl 0.2 M EDTA and 10 µl 0.1 M NaF, was added to extract inositol phosphates. The whole TCA precipitate was suspended, transferred to an ice-cold micro tube, vortexed, and frozen twice in liquid nitrogen. Precipitated protein was removed by centrifugation (5 min; 4,000 rpm; 4 °C) and the supernatant was incubated at 37 °C for 15 min to hydrolyze creatine phosphate. Supernatants were extracted three times with diethyl ether and neutralized to pH 6 to 7 with 2 to 4 µl 2 M Tris-base. Ether was removed by lyophylization and from the re-dissolved pellets nucleotides were removed by extraction with charcoal. Inositol phosphates were analyzed by micro-metal dye detection HPLC (MDD-HPLC) [22,23].

Ca^{2+} measurements and ratiometric Ca^{2+}-imaging

Ca^{2+} measurement in suspended cells was performed as described in [26]. For ratiometric Ca^{2+}-imaging 2.5×10^5 cells were loaded with fura-2/AM (4 µg/ml) for 30 min at 37 °C in buffer A containing 140 mM NaCl, 5 mM KCl, 1 mM $MgSO_4$, 1 mM $CaCl_2$, 1 mM Na_2HPO_4, 5.5 mM glucose, and 20 mM HEPES (pH 7.4) as described [27], washed twice with buffer A and kept in the dark at room temperature until use. 8 well µ-Slides (Ibidi, Munich, Germany) were first coated with 50 µl ECM and subsequently covered with 100 µl buffer A. 100 µl cell suspension (2.5×10^5 cells/ml) were added

and the slide was mounted on stage of a fluorescence microscope (Leica DMIRE2). Ratiometric Ca^{2+} imaging was performed as described [27]. We used an Improvision imaging system (Tübingen, Germany) built around the Leica microscope at 100-fold magnification. Illumination at 340 and 380 nm was carried out using a monochromator system (Polychrom IV, TILL Photonics, Gräfelfing, Germany). Images were taken with a gray-scale CCD-camera (type C 4742-95-12ER; Hamamatsu, Enfield, United Kingdom) operated in 8-bit mode. The spatial resolution was 512 x 640 pixel at 100-fold magnification. Camera exposure times were 21 ms (at 340 nm) and 7 ms (at 380 nm). The acquisition rate was adjusted to ~12 ratios per minute. Raw data images were stored on hard disk. Confocal Ca^{2+} images were obtained by off-line deconvolution (no-neighbor algorithm) using the volume deconvolution module of the Openlab software as described recently for 3T3 fibroblasts [27]. The deconvolved images were used to construct ratio images (340/380 nm) pixel by pixel. Finally, ratio values were converted into Ca^{2+} concentrations by external calibration [28]. Data processing was performed using Openlab software, version 4.0.4 [Improvision, Tübingen, Germany).

RESULTS

Transient overexpression of IP3K-A in H1299 cells induced formation of branching protrusions.

To investigate the cellular effects of increased expression of IP3K-A, we used the cell line H1299 as model. To increase and to monitor IP3K-A expression, a GFP-IP3K-A fusion protein was transiently overexpressed in H1299 cells. 24 h after transfection expression levels of endogenous IP3K-A and GFP-IP3K-A were examined by Western-blot using IP3K-A specific antibodies.

As shown in Figure 1A (left panel) the cells expressed high levels of GFP-IP3K-A. In addition a strong signal of a band corresponding to the molecular weight (MW) of IP3K-A was observed, which might be due to up-regulation of endogenous IP3K-A or to degradation of the GFP-IP3K-A fusion protein to GFP and IP3K-A. Therefore expression of GFP was analyzed using a GFP specific antibody (Fig. 1A right panel). Since we detected a strong signal at 28 kD, which corresponds to the molecular mass of GFP, we assume that the strong signal observed at 52 kD corresponds to a degradation product of the GFP-IP3K-A fusion protein.

To analyze the effect of IP3K-A overexpression on cell morphology, GFP fluorescence of the fusion protein or of GFP alone (control) was monitored by fluorescence microscopy. Control cells had a fusiform or round/oval shaped morphology and the cells extended many small filopodia. Cells strongly overexpressing IP3K-A formed long branching protrusions and exhibited a similar cell body as control cells (Fig.1B). Most of the cells overexpressing IP3K-A formed many branching filopodia (43%) exhibiting approximately the same length as the cell body, or few branching lamellipodia or filopodia longer than the cell body (38%) (Fig. 1C). In contrast, only very few control cells extended many branching filopodia (5%) and no formation of long branching filopodia or lamellipodia were detected (Fig. 1C) (for definition of filopodia and lamellipodia, see [29]).

Transient overexpression of IP3K-B and IP3K-C GFP-fusion proteins did not alter cell morphology (data not shown). These data clearly reveal that only overexpression of IP3K isoform A induces the formation of extended branching protrusions in H1299 cells.

Stable overexpression of IP3K-A altered the cytoskeleton and increased invasive migration of H1299 cells without affecting proliferation

Since it is known that the ability to form filopodia and lamellipodia facilitates cell motility [29], we examined the impact of increased IP3K-A expression on cell motility. These experiments require homologous cell populations, thus it was necessary to establish cell clones stably overexpressing IP3K-A. Therefore, H1299 cells stably overexpressing GFP-IP3K-A or GFP were generated and four cell clones (#6, #7, #8, and #10) with similar IP3K-A overexpression were selected. Cell clones expressing GFP alone were used as control.

To examine the influence of IP3K-A overexpression on cell growth behaviour, the cell clones were cultivated under three-dimensional cell culture conditions, in porous capillaries permeable for growth medium (Fig. 2A). To exclude clonal effects, all four clones as well as wt H1299 cells were examined. Control and wt cells formed epithelial-like dense cell colonies. In contrast, H1299 cells overexpressing IP3K-A strongly attached to the wall of the capillary. They grew in a dispersed fibroblast-like manner and formed long protrusions (see arrows in Fig. 2A) as also observed in cells transiently overexpressing IP3K-A. In addition, these experiments reveal that IP3K-A expression increases motility of H1299 cells. Since we did not find differences between the four cell clones, continuative experiments were performed only with one clone which was designed as H1299-IP3K-A. Control cells were named H1299-GFP. Expression levels of endogenous IP3K-A and of the GFP-IP3K-A fusion protein are depicted in Fig. 2B. The Figure shows strong overexpression of the GFP-IP3K-A protein and reveals that the intensity of the band corresponding to the MW of endogenous IP3K-A was increased again in H1299-IP3K-A cells. The stably overexpressed GFP-IP3K-A fusion protein also showed strong degradation of GFP (data not shown), thus

the band of 52 MW might correspond to a degradation product of the GFP-IP3K-A fusion protein.

The observed morphological changes of H1299-IP3K-A cells indicated that IP3K-A expression altered the cytoskeleton of the cells. To analyze if IP3K-A influences the F-actin structure, H1299-IP3K-A and control cells, cultivated in chamber slides, were stained with FITC phalloidin to visualize F-actin. As shown in Figure 3 control cells formed distinct actin stress fibers. In contrast, in H1299-IP3K-A cells no formation of actin stress fibers was observed, but most of the F-actin was distributed around the cell periphery and in protrusions.

Next, we analyzed the impact of IP3K-A overexpression on invasive cell migration, using the Boyden chamber assay. In this assay migration through extracellular matrix (ECM, derived from the Engelbreth-Holm-Swarm mouse sarcoma) and through filters of 3 µm pore size is measured. As shown in Figure 4A, an about 2-fold increase ($p<0.001$, t-test) in invasive ability was observed in H1299-IP3K-A cells as compared to controls. To determine if IP3K-A expression also affects proliferation, cell growth was measured by cell counting using the CASY-1 cell counter (Fig. 4B). No difference was found between control and H1299-IP3K-A cells. In conclusion, these results show that IP3K-A expression alters the cytoskeleton and increases invasive in vitro migration of H1299 cells without affecting proliferation.

IP3K-A overexpression promoted the mesenchymal phenotype of H1299 cells

Based on the phenotypic differences between H1299-IP3K-A and control cells we speculated that overexpressing of IP3K-A in H1299 cells resulted in a mesenchymal phenotype. Consequently, we examined expression of the mesenchymal marker proteins N-cadherin and vimentin by immunoblot analysis. Expression of vimentin was significantly increased in cells overexpressing IP3K-A compared to control cells. N-

cadherin expression was very low in control cells and about 5-fold increased in H1299-IP3K-A cells (Fig. 5A). To exclude that increased expression of vimentin and N-cadherin is a consequence of unspecific clonal effects, expression of these proteins was analyzed in further cell clones overexpressing IP3K-A (clone #6, #7 and #10, see Fig. 2A). These cell clones also showed increased expression of vimentin and N-cadherin, compared to control cells (data not shown). In addition expression of abundant cellular proteins involved in signal transduction (Fig. 5B, left panel) and/or in actin remodeling (Fig. 5B, right panel) was examined; GAPDH and actin served as loading controls. Since we did not find significant differences between control and H1299-IP3K-A cells, and found up-regulation of vimentin and N-cadherin in three further cell clones overexpressing IP3K-A, we assume that increased expression of the mesenchymal proteins is a specific effect of overexpression of IP3K-A.

IP3K-A induced cell migration was not dependent on calcium signaling

The results above demonstrate that increased expression of IP3K-A increases motility and invasive migration of H1299 cells. Elevated Ca^{2+} concentrations can stimulate cell migration [28] and one important cellular effect of IP3K-A activity is to regulate intracellular Ca^{2+}concentrations ($[Ca^{2+}]_i$) by conversion of the calcium mobilizing second messenger Ins(1,4,5)P_3. Therefore the effect of IP3K-A overexpression on $[Ca^{2+}]_i$ was measured. H1299-IP3K-A and control cells were loaded with Fura-2, and stimulated with 100 µM ATP to stimulate purinergic P2Y receptors. Using a Ca^{2+}-free/Ca^{2+}-readdition protocol [26], we found that, compared to control cells, in H1299-IP3K-A cells calcium release was reduced by about 75% and calcium influx by about 50% (Fig. 6A). Thus it is unlikely that increased migration of H1299-IP3K-A cells is dependent on calcium signals.

To verify this assumption, $[Ca^{2+}]_i$ in cells that adhere or migrate through ECM was analyzed by confocal calcium imaging. Fura-2 loaded H1299-IP3K-A and control cells were supplied to ECM covered slides and $[Ca^{2+}]_i$ and morphology of the same cells were monitored for 20 min by fluorescence and light microscopy. As shown in Figure 6B (upper panel) the cell shape of control cells remained unchanged during the experiment. In contrast, H1299-IP3K-A cells changed their morphology: they formed small protrusion and started to migrate into the ECM (Fig. 6B lower panel). Despite these morphological changes and induction of migration, neither in these nor in control cells calcium signals were observed. As a positive control, carried out under the same experimental conditions, transient calcium signals were induced by ATP in both cell types (data not shown). The fact that in unstimulated H1299-IP3K-A cells, migrating through ECM, no calcium signal was observed suggests that IP3K-A induced increase of invasive cell migration is not dependent on calcium signaling.

IP3K-A overexpression altered intracellular inositol phosphate concentrations

Recently, it has been reported that increased levels of the IP3K product Ins(1,3,4,5)P_4 can stimulate the Ras-ERK pathway through binding of Ras-GAP [6]. In cells with low Ins(1,3,4,5)P_4 concentrations Ras-GAP is bound to PtdIns(4,5)P_2 resulting in inactivation of Ras. Increased Ins(1,3,4,5)P_4 levels can compete for binding to PtdIns(4,5)P_2 and Ras-GAP translocates to the cytosol, abolishing inactivation of Ras. Since activation of the Ras-ERK pathway, can be involved in the regulation of cell motility [28], InsP concentrations in H1299-IP3K-A and control cells were analyzed by MDD-HPLC (Fig. 7A). We found significantly decreased levels of the IP3K-A substrate, Ins(1,4,5)P_3 (about 2-fold, $p<0.01$, t-test), and significant increased levels of the product Ins(1,3,4,5)P_4 (about 4-fold, $p<0.1$, t-test) in cells overexpressing IP3K-A compared to control cells. However, no increased concentrations of further higher phosphorylated

inositols were detected. In contrast, significant decreased levels of Ins(1,2,3,4,5)P_5 (about 3-fold, $p<0.1$, t-test) and of InsP_6 (about 20%, $p<0.01$, t-test) were found.

Since overexpression of IP3K-A significantly increased the concentration of Ins(1,3,4,5)P_4, activation of ERK1/2 in H1299-IP3K-A cells in comparison to control cells was examined. In addition, we analyzed the intracellular distribution of GAP^1 by immunocytology using a specific GAP^1 antibody. In both, control and H1299-IP3K-A cells GAP^1 was mainly located in the cytoplasm and within the nucleus (Fig. 7B). Furthermore, high levels of pERK1/2 were found in both cell types and no difference in activation was observed (Fig. 7C). Based on these data we conclude that ERK1/2 is constitutively activated in these cells, but is not further stimulated by increased IP3K-A expression. Thus, IP3K-A induced increase of cell migration is not dependent on Ins(1,3,4,5)P_4 mediated up-regulation of ERK1/2 activity.

Transient overexpression of mutated forms of GFP-IP3K-A

To further analyze the mechanism underlying IP3K-A induced effects on cell morphology and migration, we examined if kinase activity is required. Therefore, a mutated IP3K-A form devoid of enzyme activity was produced. According to Communi et al (1993) [31] who found that exchange of D414 to N abolishes enzyme activity of rat IP3K-A, the human homologous D416 was changed to N (mut1) in the human protein. To measure enzyme activity of wt and mutated GFP-IP3K-A fusion proteins without the background of endogenous protein, we purified the proteins by GFP-immunoprecipitation after transient overexpression in H1299 cells, and determined conversion of Ins(1,4,5)P_3 to Ins(1,3,4,5)P_4 by HPLC. We found that the wt protein exhibited an enzyme activity of 0.212 ± 0.013 µmol/mg/min while the mutated IP3K-A was catalytically inactive.

To analyze the effect of mut1 on morphology of H1299 cells, the shape of cells overexpressing the mutated protein was compared to the morphology of cells overexpressing the wt protein. Interestingly, their morphology was similar to that of cells overexpressing the IP3K-A wt enzyme (Fig. 8A). Since Western-blot analysis revealed that cells overexpressing mut1 also showed a stronger signal at 52 kD than control cells (data not shown), we examined whether endogenous IP3K-A activity might be up-regulated. In case cells overexpressing mut1 show higher IP3K-A activity than control cells, one cannot exclude that the observed morphological changes induced by overexpression of mut1 result from up-regulation of endogenous IP3K-A activity. However, we found that enzyme activity in cells overexpressing mut1 was similar to that of control cells (Fig. 8B), indicating that endogenous IP3K-A was not up-regulated. Thus enzymatic activity of IP3K-A does not seem to be required to induce morphological changes in H1299 cells.

To reveal if actin binding is necessary to induce the formation of branching filopodia, the actin binding domain (ABD) was deleted and the mutated protein (mut2: aa 67 – 461, ΔABD) was overexpressed in H1299 cells. As shown in Figure 8C no morphological differences between control cells and cells overexpressing mut2 were visible. Thus, actin binding of IP3K-A is required to induce phenotypic changes. Next, the effect of overexpression of the ABD alone (mut3: aa 1-66, ABD) was analyzed. This fragment also did not induce the same effect as observed for the full length protein (Fig. 8C). To exclude that the effects on cell morphology induced by mut1 are due to the fact that mut1 shows stronger overexpression than mut2 and mut3, expression levels of these proteins were analyzed by Western-blot using GFP specific antibodies. As shown in Figure 8D, expression of mut2 and mut3 was even stronger than expression of mut1 whereby mut2 showed strong degradation.

Taken together the results show that actin localization of IP3K-A is required to induce formation of branching protrusions, and reveal that the IP3K-A induced effects on cell motility are not due to enzymatic activity. Since only overexpression of the full length protein induced morphological changes, we exclude the possibility that the observed effects are overexpression artefacts.

DISCUSSION

In this study, we used a cellular model to examine the phenotypic consequences of high expression of IP3K-A. We found that overexpression of the protein in H1299 cells induced marked morphological changes through reorganization of the actin cytoskeleton. In contrast to control cells which formed distinct actin stress fibers, cells overexpressing IP3K-A failed to form stress fibers, but showed cortical actin filaments which accumulated in cellular protrusions. Only these cells extended long branching protrusions and grew in a dispersed manner. Furthermore, they expressed increased levels of the mesenchymal marker proteins vimentin and N-cadherin. Most likely due to these phenotypic changes, cells overexpressing IP3K-A showed increased motility and migration in vitro as compared to control cells.

To elucidate the mechanism by which IP3K-A increases migration of H1299 cells, we first investigated the potential effects of enhanced IP3K-A activity, i.e. altered calcium and InsPs signaling. However, these data gave no clear evidence that IP3K-A induced phenotypic changes of H1299 cells are due to enzymatic activity. Therefore, we examined the effect of overexpression of a kinase-dead mutant on morphology of H1299 cells. Indeed, we found that a protein devoid of enzyme activity induced similar morphological changes as observed for the wt protein, indicating that the IP3K-A induced effects on cell morphology are due to non-enzymatic activities of the protein. For some inositol phosphate kinases it has already been shown that they regulate cellular

processes by protein-protein interactions. Yeast inositol phosphate multikinase interacts with the transcriptional complex ArgR-Mcm1, whereby it serves as a molecular chaperone resulting in stimulation of mRNA export [32]. Furthermore, it was previously shown that inositol pentakisphosphate 2-kinase is a component of stress granules where it co-localizes with cytosolic mRNA and the stress granule marker proteins poly(A) binding protein (PABP) and TIA1 related protein (TIAR). Therefore the kinase might be involved in stress recovery [33]. In addition co-immunoprecipitation studied revealed that inositol hexakisphosphate kinase-2 (IP6K-2) interacts with tumor necrosis factor receptor-associated factor 2 (TRAF 2) through which it mediates attenuation of nuclear factor-kappa B (NFκB) induced signaling [34]. These studies show that the cellular effects induced by inositol phosphate kinases are not only due to their enzymatic activities, but are additionally mediated by direct protein-protein interactions. Our result that enzyme activity of IP3K-A was not required to induce branching protrusions indicates that also IP3K-A regulates cellular processes through protein-protein interactions. Since actin localization of IP3K-A was necessary to change morphology of H1299 cells, the protein might be directly involved in actin polymerization or recruits proteins to actin that mediate actin remodeling. However, the molecular mechanisms how IP3K-A induces formation of branching protrusions deserves further investigations.

ACKNOWLEDGEMENT

We thank Prof. Schumacher for help with cultivating cells in medium permeable capillaries. This project was supported by the Roggenbuck Stiftung and by the Universitätsklinikum Hamburg-Eppendorf, Forschungsförderungsfonds Medizin.

REFERENCES

1 Irvine R.F., Lloyd-Burton S.M., Yu J.C., Letcher A.J., Schell M.J. (2006) The regulation and function of inositol 1,4,5-trisphosphate 3-kinases. Adv. Enzyme Regul. **46**, 314-23

2 Hashii M., Nakashima S., Yokoyama S., Enomoto K., Minabe Y., Nozawa Y., Higashida H. (1996) Bradykinin B2 receptor-induced and inositol tetrakisphosphate-evoked Ca2+ entry is sensitive to a protein tyrosine phosphorylation inhibitor in ras-transformed NIH/3T3 fibroblasts. Biochem J. **319**, 649-56

3 Hermosura M.C., Takeuchi H., Fleig A., Riley A.M., Potter B.V., Hirata M., Penner R. (2000) InsP4 facilitates store-operated calcium influx by inhibition of InsP3 5-phosphatase. Nature **408**, 735-40

4 Miller A.T., Sandberg M., Huang Y.H., Young M., Sutton S., Sauer K., Cooke M.P. (2007) Production of Ins(1,3,4,5)P4 mediated by the kinase Itpkb inhibits store-operated calcium channels and regulates B cell selection and activation. Nat Immunol **8**, 514-21

5 Cullen P.J., Hsuan J.J., Truong O., Letcher A.J., Jackson T.R., Dawson A.P., Irvine R.F. (1995) Identification of a specific Ins(1,3,4,5)P4-binding protein as a member of the GAP1 family. Nature **376**, 527-30

6 Maréchal Y., Pesesse X., Jia Y., Pouillon V., Pérez-Morga D., Daniel J., Izui S., Cullen P.J., Leo O., Luo H.R., Erneux C., Schurmans S. (2007) Inositol 1,3,4,5-tetrakisphosphate controls proapoptotic Bim gene expression and survival in B cells. Proc. Natl. Acad. Sci. U S A **104**, 13978-83

7 Huang Y.H., Grasis J.A., Miller A.T., Xu R., Soonthornvacharin S., Andreotti A.H., Tsoukas C.D., Cooke M.P., Sauer K. (2007) Positive regulation of Itk PH domain function by soluble IP4. Science **316**, 886-89

8 Shears S.B. (2004) How versatile are inositol phosphate kinases? Biochem. J. **377**, 265-80

9 Dewaste V., Roymans D., Moreau C., Erneux C. (2002) Cloning and expression of a full-length cDNA encoding human inositol 1,4,5-trisphosphate 3-kinase B. Biochem Biophys. Res. Commun. **291** 400-5

10 Nalaskowski M.M., Bertsch U., Fanick W., Stockebrand M.C., Schmale H., Mayr G.W. (2003) Rat inositol 1,4,5-trisphosphate 3-kinase C is enzymatically specialized for basal cellular inositol trisphosphate phosphorylation and shuttles actively between nucleus and cytoplasm. J. Biol. Chem. **278,** 19765-76

11 Vanweyenberg V., Communi D., D'Santos C.S., Erneux C. (1995) Tissue- and cell-specific expression of Ins(1,4,5)P_3 3-kinase isoenzymes. Biochem. J. **306**, 429-35

12 Wen B.G., Pletcher M.T., Warashina M., Choe S.H., Ziaee N., Wiltshire T., Sauer K., Cooke M.P. Inositol (1,4,5) trisphosphate 3 kinase B controls positive selection of T cells and modulates Erk activity. (2004) Proc. Natl. Acad. Sci. U S A. **101**, 5604-9.

13 Onouchi Y., Gunji T., Burns J.C., Shimizu C., Newburger J.W., Yashiro M., Nakamura Y., Yanagawa H., Wakui K., Fukushima Y., Kishi F., Hamamoto K., Terai M., Sato Y., Ouchi K,. Saji T., Nariai A., Kaburagi Y., Yoshikawa T., Suzuki K., Tanaka

T., Nagai T., Cho H., Fujino A., Sekine A., Nakamichi R., Tsunoda T., Kawasaki T., Nakamura Y., Hata A. (2008) ITPKC functional polymorphism associated with Kawasaki disease susceptibility andformation of coronary artery aneurysms. Nat Genet. **40**, 35-42

14 Schell M.J., Erneux C., and Irvine R.F. (2001) Inositol 1,4,5-trisphosphate 3-kinase A associates with F-actin and dendritic spines via its N terminus J. Biol. Chem. **276**, 37537-46

15 Schell M.J., Irvine R.F. (2006) Calcium-triggered exit of F-actin and IP(3) 3-kinase A from dendritic spines is rapid and reversible. Eur. J. Neurosci. **24**, 2491-503

16 Moon K.H., Lee S.Y., Rhee S.G. (1989) Developmental changes in the activities of phospholipase c, 3-kinase, and 5-phosphatase in rat brain.Biochem Biophys Res Commun.**164**, 370-4.

17 Mailleux P., Takazawa K., Erneux C., Vanderhaeghen J.J. (1993) Distribution of the neurons containing inositol 1,4,5-trisphosphate 3-kinase and its messenger RNA in the developing rat brain. Comp Neurol. **327**, 618-29

18 Kim I.H., Park S.K., Sun W., Kang Y., Kim H.T., Kim H. (2004) Spatial learning enhances the expression of inositol 1,4,5-trisphosphate 3-kinase A in the hippocampal formation of rat. Brain. Res. Mol. Brain. Res. **124**, 12-9

19 Jun K., Choi G., Yang S.G., Choi K.Y., Kim H., Chan G.C., Storm D.R., Albert C., Mayr G.W., Lee C.J., Shin H.S. (1998) Enhanced hippocampal CA1 LTP but normal spatial learning in inositol 1,4,5-trisphosphate 3-kinase(A)-deficient mice. Learn. Mem. **5**, 317-30.

20 Chakrabarti R., Schutt C.E. (2002) Novel sulfoxides facilitate GC-rich template amplification. Biotechniques. **866**, 870-2

21 Wang W. Malcolm B.A. (1999) Two-stage PCR protocol allowing introduction of multiple mutations, deletions and insertions using QuikChange Site-Directed Mutagenesis. Biotechniques **26**, 680-2

22 Mayr G.W. (1988) A novel metal-dye detection system permits picomolar-range h.p.l.c. analysis of inositol polyphosphates from non-radioactively labelled cell or tissue specimens. Biochem. J. **254**, 585-91

23 Guse A.H., Goldwich A., Weber K., Mayr G.W. (1995). Non-radioactive, isomer-specific inositol phosphate mass determinations: high-performance liquid chromatography-micro-metal-dye detection strongly improves speed and sensitivity of analyses from cells and micro-enzyme assays. J. Chromatogr. B. Biomed. Appl. **672**, 189 -98

24 Nalaskowski M.M., Windhorst S., Stockebrand M.C., Mayr G.W. (2006) Subcellular localisation of human inositol 1,4,5-trisphosphate 3-kinase C: species-specific use of alternative export sites for nucleo-cytoplasmic shuttling indicates divergent roles of the catalytic and N-terminal domains. Biol. Chem. **387**, 583-93

25 Hohenberg H., Mannweiler K., Muller M. (1994) High-pressure freezing of cell suspensions in cellulose capillary tubes. J Microsc **175**, 34-3

26 Guse, A. H., Roth, E., and Emmrich, F. (1993) Intracellular Ca2+ pools in Jurkat T-lymphocytes. Biochem. J. **291**, 447-51

27 Kunerth, S., Mayr, G. W., Koch-Nolte, F., and Guse, A.H. (2003) Analysis of sub-cellular calcium signals in T-lymphocytes. Cell Signal. **15**, 783-92

28 Bruzzone, S., Kunerth, S., Zocchi, E., De Flora, A., and Guse, A. H. (2003) Spatio-temporal propagation of Ca2+ signals by cyclic ADP-ribose in 3T3 cells stimulated via purinergic P2Y receptors. J. Cell Biol. **163**, 837-45

29 Ridley A.J. (2006) Rho GTPases and actin dynamics in membrane protrusions and vesicle trafficking. Trends Cell Biol. **16**, 522-9

30 Feldner J.C., Brandt B.H. (2002) Cancer cell motility--on the road from c-erbB-2 receptor steered signaling to actin reorganization. Exp. Cell Res. **272**, 93-108

31 Communi D., Vanweyenberg V., Erneux C. (1995) Molecular study and regulation of D-myo-inositol 1,4,5-trisphosphate 3-kinase. Cell Signal. **7**: 643-650

32 Odom A.R., Stahlberg A., Wente S.R. York JD. (2000)A role for nuclear inositol 1,4,5-trisphosphate kinase in transcriptional control. Science **287,** 2026-9.

33 Brehm M.A., Schenk T.M., Zhou X., Fanick W., Lin H., Windhorst S., Nalaskowski M.M.,Kobras M., Shears S.B., Mayr G.W.(2007) Intracellular localization of human Ins(1,3,4,5,6)P5 2-kinase. Biochem. J. **408**, 335-45

34 Morrison B.H., Bauer J.A., Lupica J.A., Tang Z., Schmidt H., DiDonato J.A., Lindner D.J.(2007) Effect of inositol hexakisphosphate kinase 2 on transforming growth factor beta-activated kinase 1 and NF-kappaB activation. J. Biol. Chem. **282**, 15349-5

FIGURE LEGENDS

Figure 1 Transient overexpression of a GFP-IP3K-A fusion protein in H1299 cells induces formation of branching protrusions

(A) Total cell lysate was prepared from cells transiently overexpressing GFP-IP3K-A or GFP. 50 µg protein were subjected to SDS-PAGE followed by immunoblot analysis using a specific antibody against IP3K-A (left panel) or against GFP (right panel), and secondary peroxidase-linked antibodies. The signal intensity was analyzed by a luminescent image analyzer (model LAS-3000 plus, Fuji Film). (B) Cells were seeded in chamber slides and grown to 50% confluence. Then, the cells were transfected with a plasmid encoding for GFP (pEGFP-C1) or for a GFP-IP3K-A fusion protein using Lipofectamine as transfection reagent. After 24 h of incubation the GFP fluorescence was monitored by fluorescence microscopy. (C) The cell morphology of 100 cells overexpressing GFP or GFP-IP3K-A was monitored by light and by fluorescence microscopy and the cell type was determined. This experiment was repeated and the percentage of each cell type calculated.

Figure 2 Stable overexpression of IP3K-A increases motility of H1299 cells

(A) Cell suspensions ($1x10^7$ cells/ml) of H1299 clones and wt cells were aspirated into medium permeable capillaries, which were placed in 6 well plates containing 2 ml medium, and cultivated for 72 h. Growth behavior of cells was monitored every 24 h by light microscopy. The digital images shown here are from cells grown for 72 h. (B) Levels of GFP-IP3K-A and IP3K-A of cell lysates prepared from H1299-IP3K-A# 8 cells and cells expressing GFP alone, were evaluated by IP3K-A blotting.

Figure 3 Overexpression IP3K-A results in cytoskeletal reorganization

Cells were seeded in chamber slides, grown to 50% confluence and fixed with paraformaldehyd. F-actin was stained with TRITC phalloidin. The red fluorescence of 200 cells was monitored by fluorescence microscopy and one representative image is shown.

Figure 4 IP3K-A overexpression increases in vitro invasion of H1299 cells but has no effect on proliferation

(A) 5000 cells per well were seeded in Boyden chambers which were previously covered with ECM proteins. Then, cells were incubated for 16 h. After removing the ECM, DAPI stained cells having permeated through the membrane were counted using immunofluorescence microscopy. Invasion was expressed as amount of cells migrated through ECM ("transmigrated cells"). Data represent mean values ± SD of four independent experiments. Significance levels are indicated by ***$p<0.001$. (B) Cells for proliferation assays were seeded in 96 well plates. Cell number was determined 24 h after seeding using the CASY-1 counter and set to 1. Further cell proliferation was determined after another 24 h and 48 h. Data represent mean values ± SD of seven independent experiments.

Figure 5 IP3K-A overexpression results in increased expression of mesenchymal marker proteins

(A) IP3K-A mediated regulation of vimentin and N-cadherin was examined by Western-blotting. The signal intensity of the corresponding bands was analyzed by a luminescent image analyzer and normalized to GAPDH signals for each lane. Data represent mean values of five different spots per sample. Significance levels are indicated by

***p<0.001, obtained by t-test. (B) To exclude that up-regulation of vimentin and N-cadherin were due to clonal effects, expression of several abundant cellular proteins was analyzed by Western-blot. GAPDH and actin served as loading controls.

Figure 6 Increased invasive migration of H1299-IP3K-A cells is not dependent on $[Ca^{2+}]_i$

(A) H1299 cells were suspended, washed in calcium-free buffer and loaded with Fura-2. Basal $[Ca^{2+}]_i$ was measured and after 200 sec ATP was added to stimulated purinergic P2Y receptors. After further 200 sec 1mM Ca^{2+} was supplied. The measurements were performed in a Hitachi F-2000 spectrofluorimeter (emission 510 nm, alternating excitations 340/380 nm). In the upper panel one representative experiment is depicted. The lower panel shows the mean from three different experiments, basal Ca^{2+} influx was subtracted from these data. (B) Suspended, Fura-2 loaded H1299-IP3K-A and control cells were supplied to ECM covered chamber slides and incubated for 20 min at room temperature in the dark. Migration through ECM was monitored by light microscopy and ratiometric Ca^{2+} imaging was performed as described in Methods. The experiment was reproduced three times and the Ca^{2+} imaging data of each cell (thin lines) as well as the mean values (bold line) are shown. Cell pictures are shown from one representative experiment. Bars, 10 µm.

Figure 7 Overexpression of IP3K-A alters concentrations of higher phosphorylated inositols but does not influence localization of GAP[1] or pERK levels

(A) Extracts of H1299-IP3K-A and H1299-GFP cells were processed as described in Methods. Inositol phosphate analysis was performed by MDD HPLC. Data represent mean values ± SD of at least four independent experiments. Significance levels are indicated by *p<0.1, **p<0.01, obtained by t-test. (B) Cells were seeded in chamber

slides, grown to 70% confluence, fixed with paraformaldehyde and permeabilized with triton X-100. Then the cells were incubated with a specific GAP[1] antibody and a TRITC labeled secondary antibody. For the same cells the GFP fluorescence (left panel) and the TRITC fluorescence (right panel) are shown. (C) pERK1/2 and ERK1/2 levels were analyzed by Western-blotting.

Figure 8 Transient overexpression of mutated GFP-IP3K-A fusion proteins in H1299 cells

(A) Cells were seeded in chamber slides and grown to 50% confluence. Then, the cells were transfected with a plasmid encoding for GFP (pEGFP-C1) or for a kinase-dead GFP-IP3K-A fusion protein (D416N) using Lipofectamine as transfection reagent. After 24 h of incubation the GFP fluorescence was monitored by fluorescence microscopy. (B) Activity of IP3K-A immunoprecipitated proteins from cells overexpressing GFP, GFP-IP3K-A or GFP-IP3K-A D416N were analyzed by MDD-HPLC and expressed as µmol/min per mg of total cell protein. (C) The same experiment as described in (A) was performed with two further mutated IP3K-A proteins: a protein lacking the ABD (ΔABD) and the ABD alone (ABD). For each mutant the cell type of 100 cells was determined and the experiment was repeated (lower panel). (D) Expression levels of mut1-3 were analyzed by Western-blot using GFP specific antibodies.

FIGURES

Figure 1

A

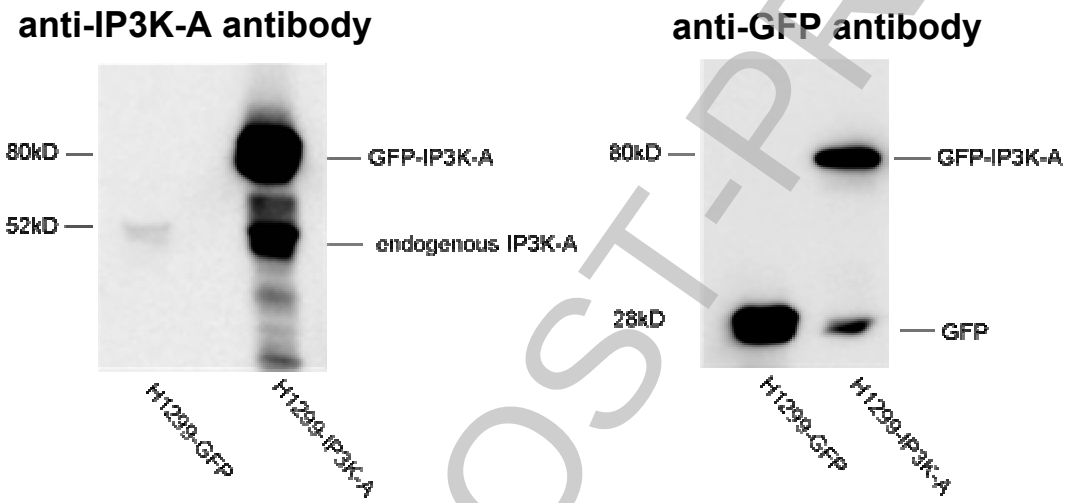

B

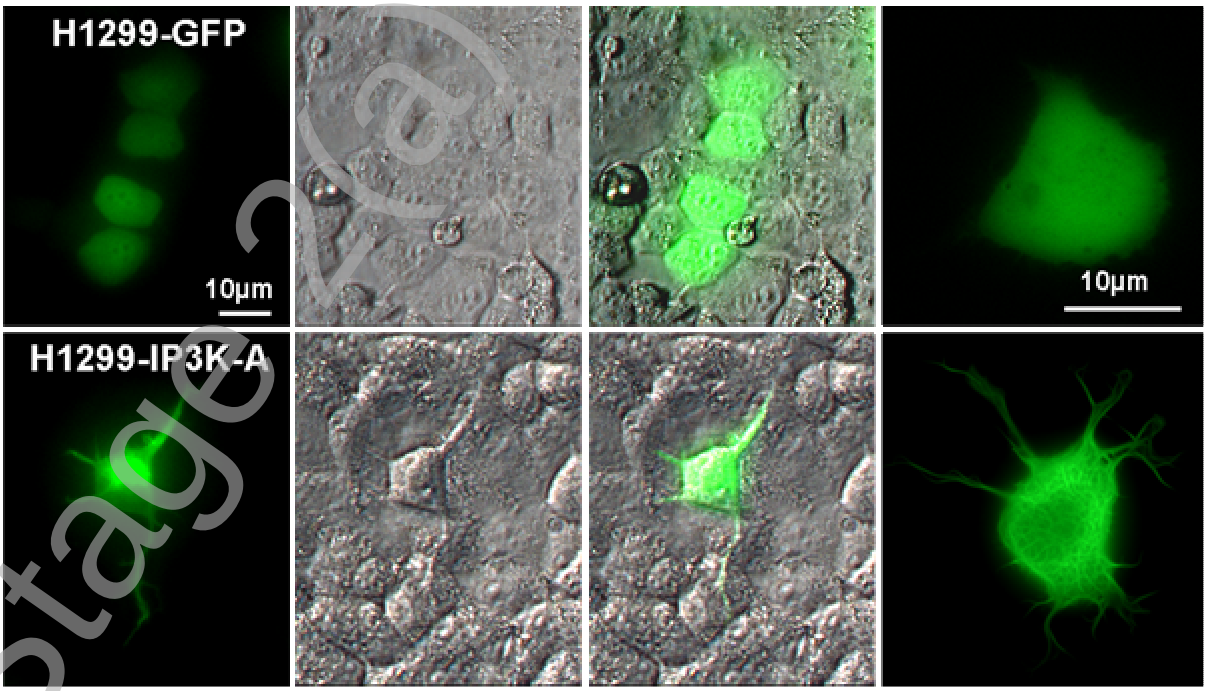

C

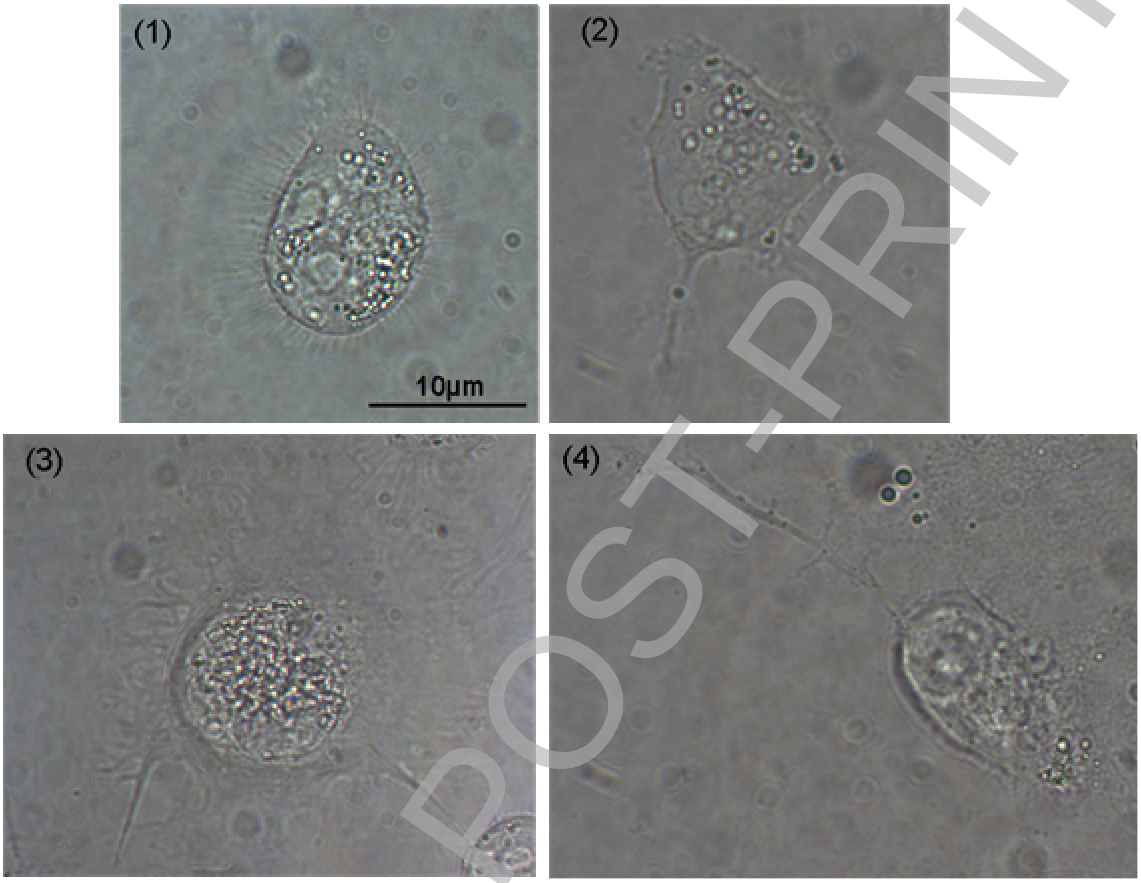

Morphology	H1299-GFP [%] cells	H1299-IP3K-A [%] cells
(1) Many short filopodia	64 ± 4	9 ± 1
(2) Few filopodia	31 ± 5	10 ± 2
(3) Many branching filopodia	5 ± 0.5	43 ± 4
(4) Few branching long filopodia or lamellipodia	none	38 ± 7

Figure 2

A

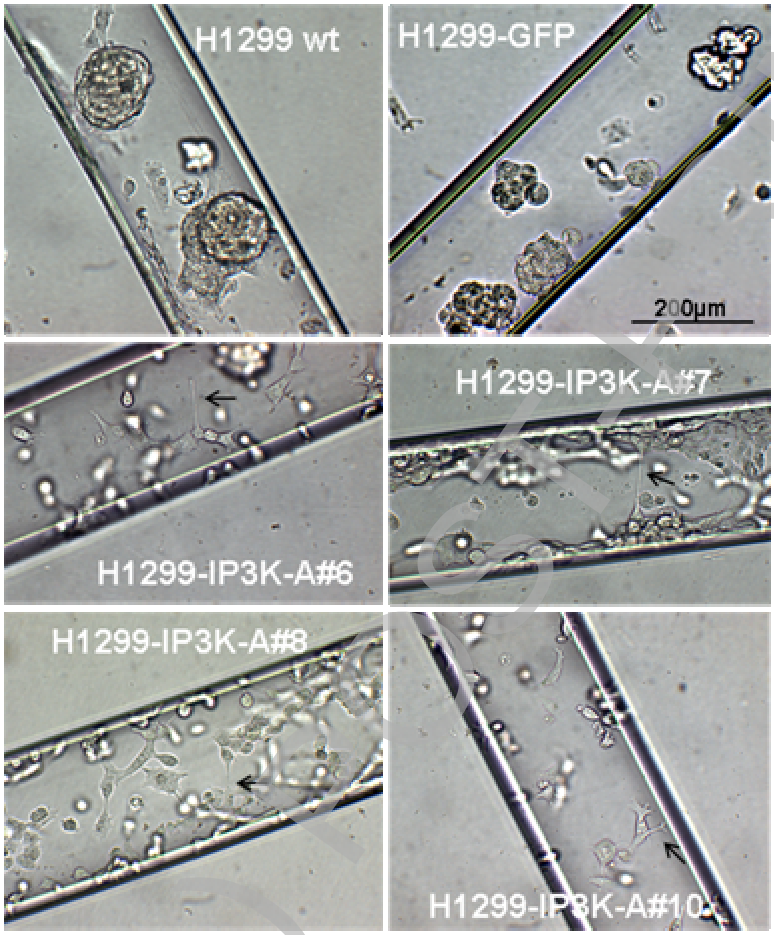

B

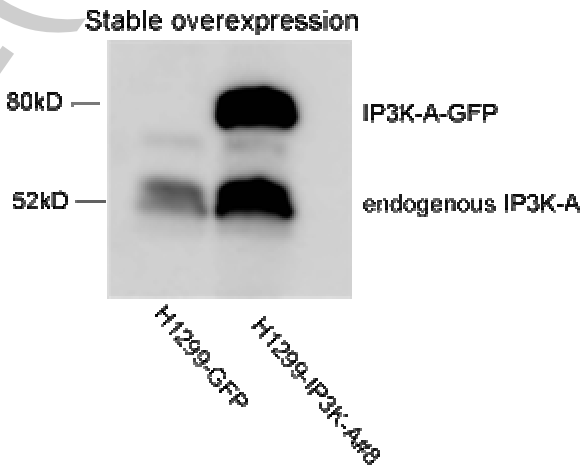

Figure 3

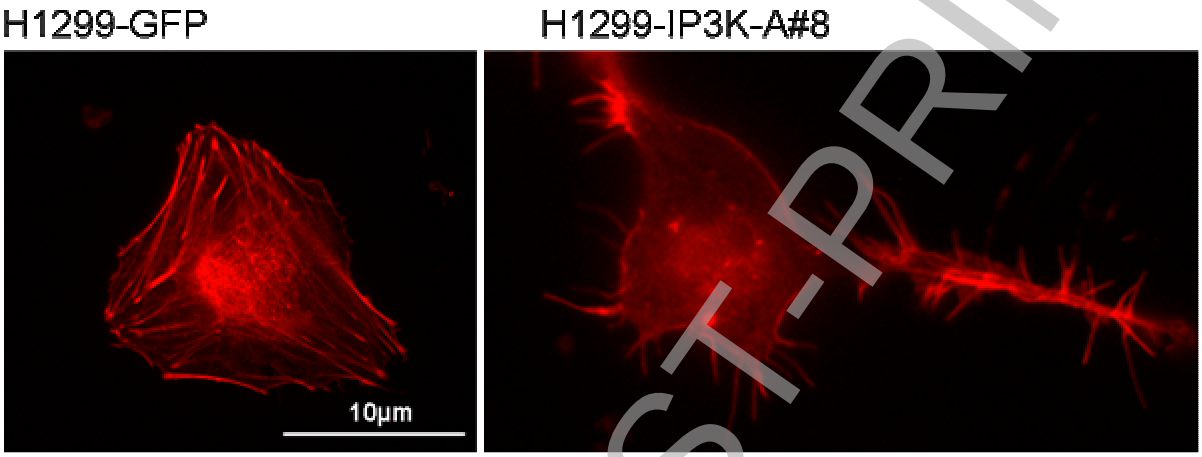

Figure 4

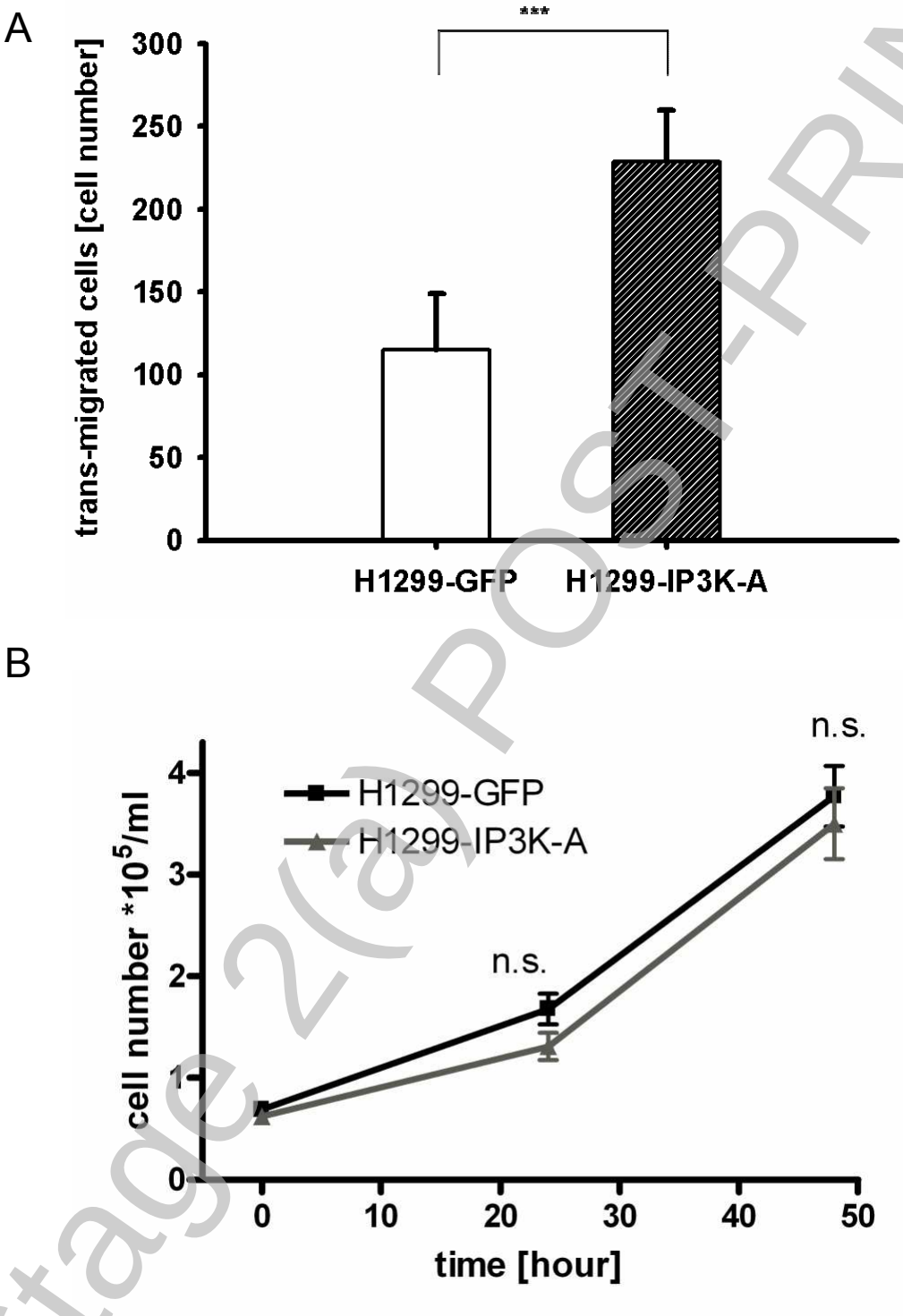

Figure 5

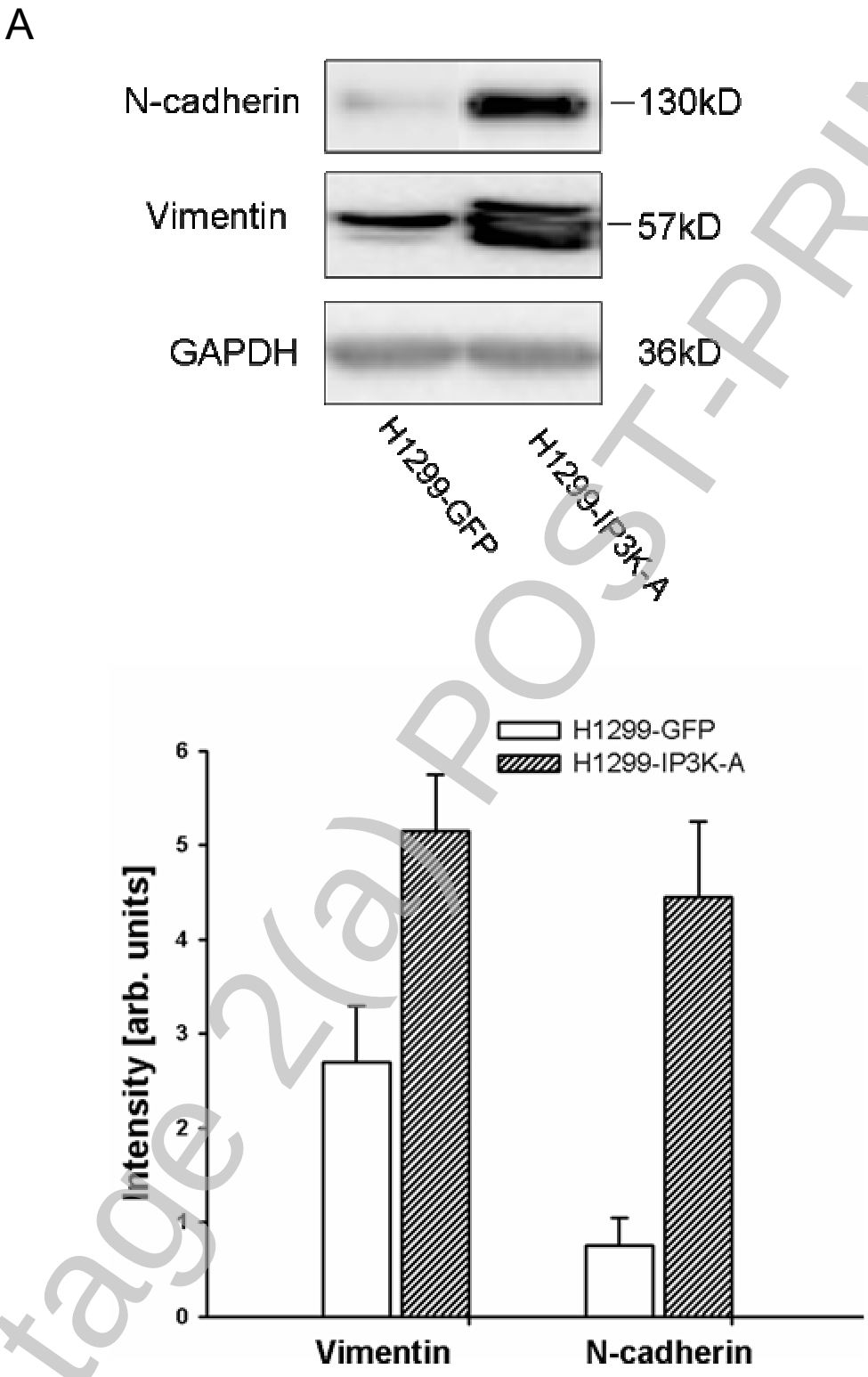

B

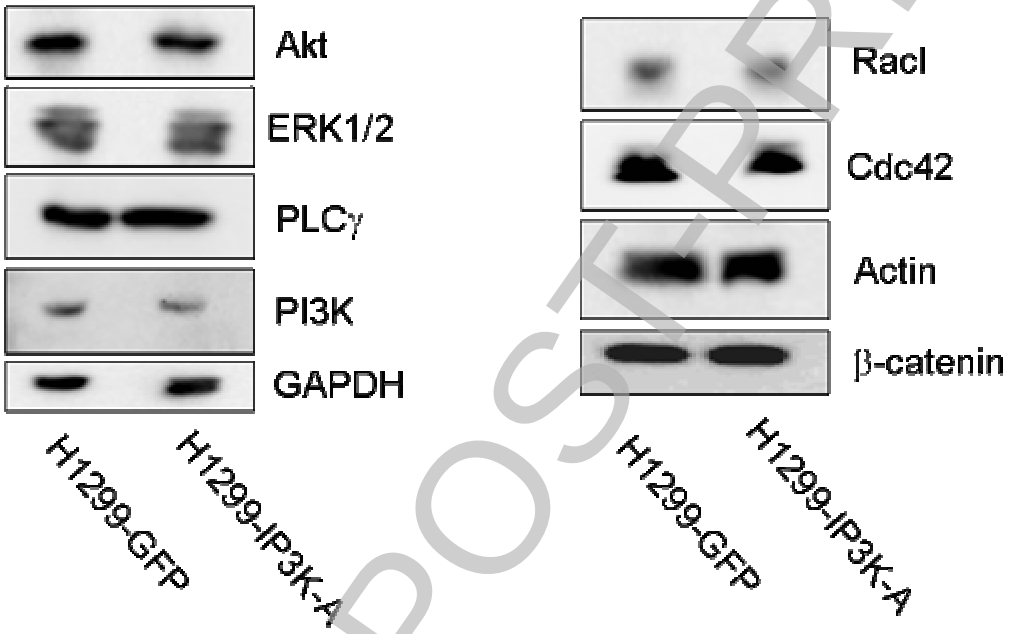

Figure 6

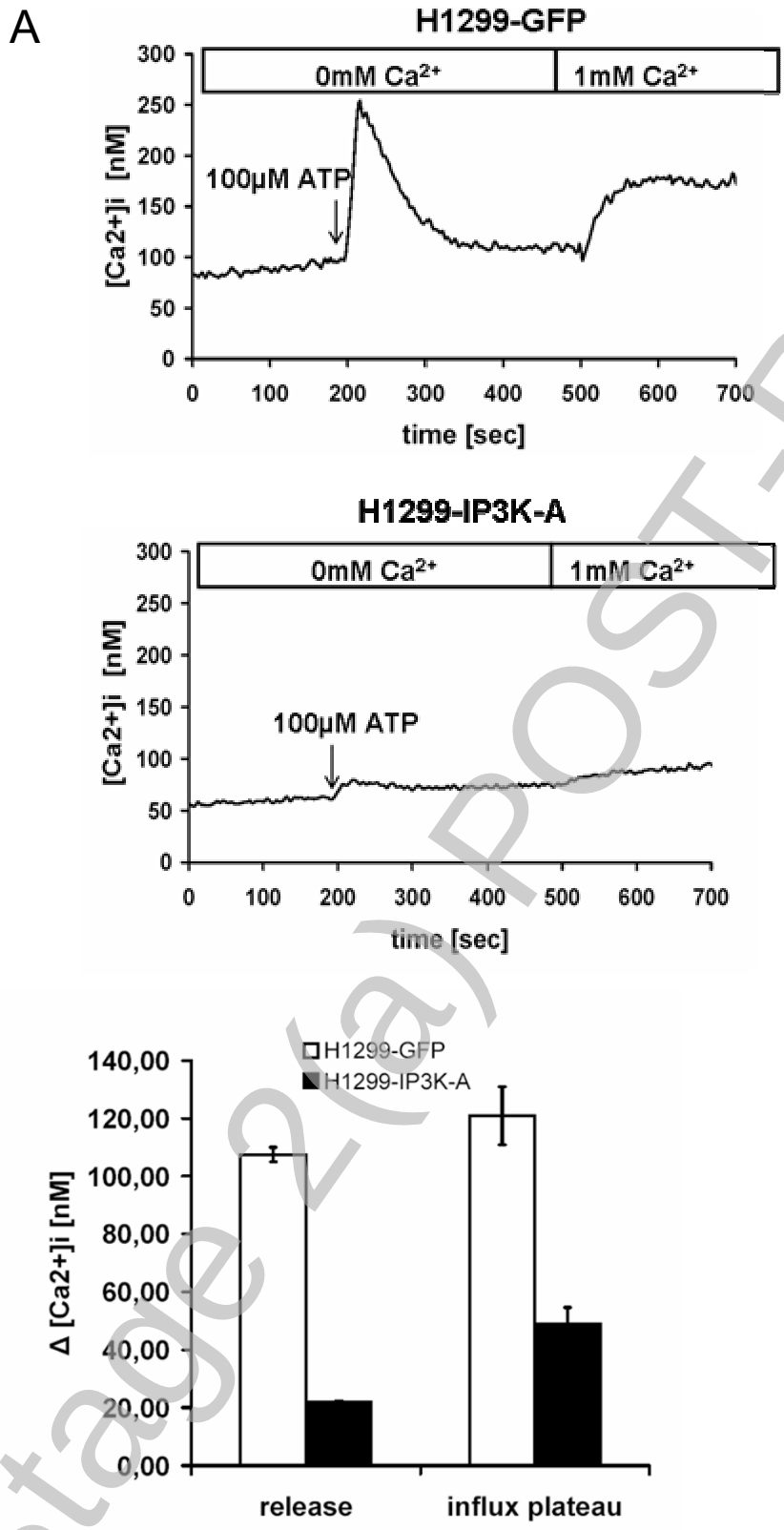

B

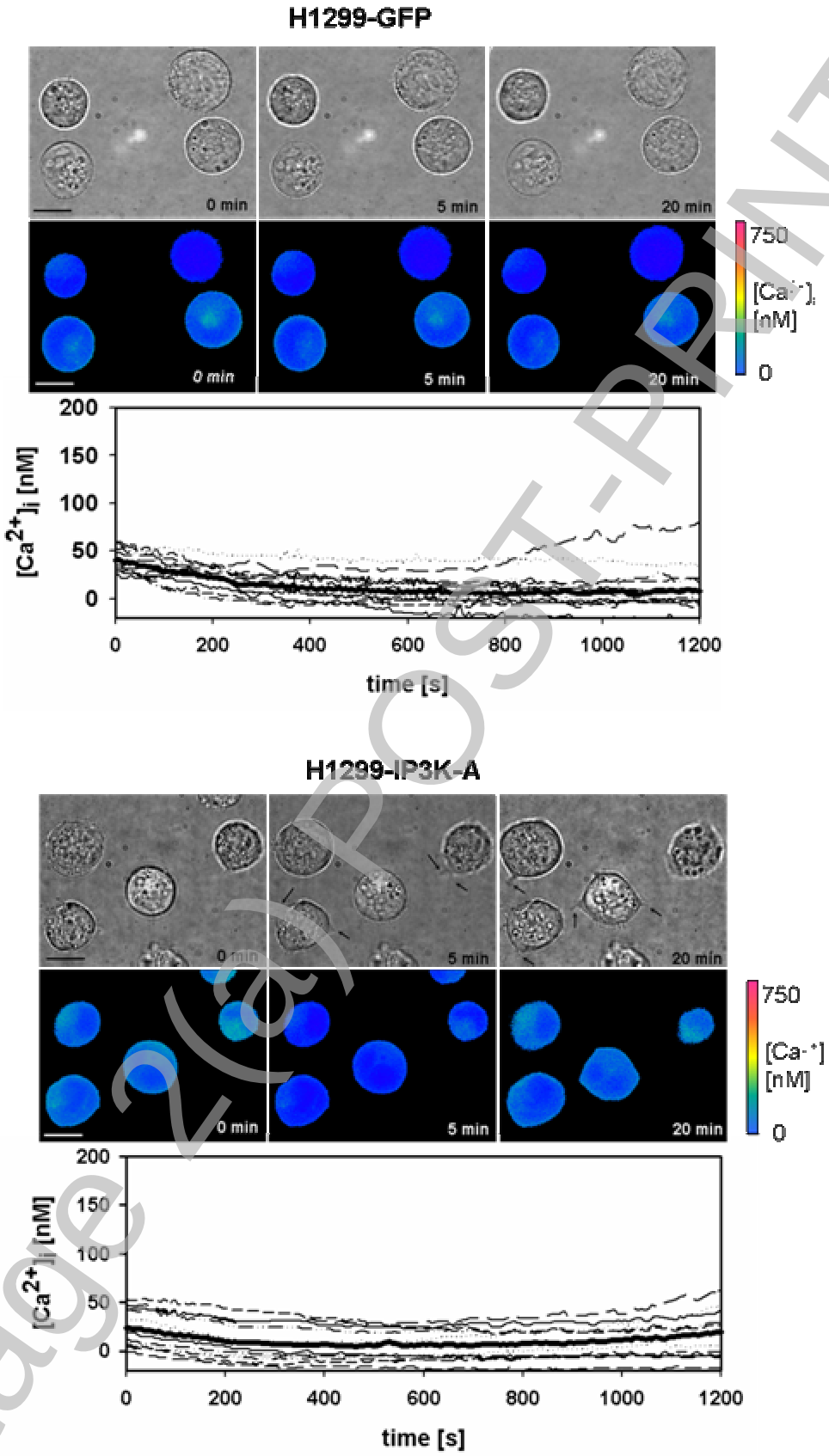

Figure 7

A

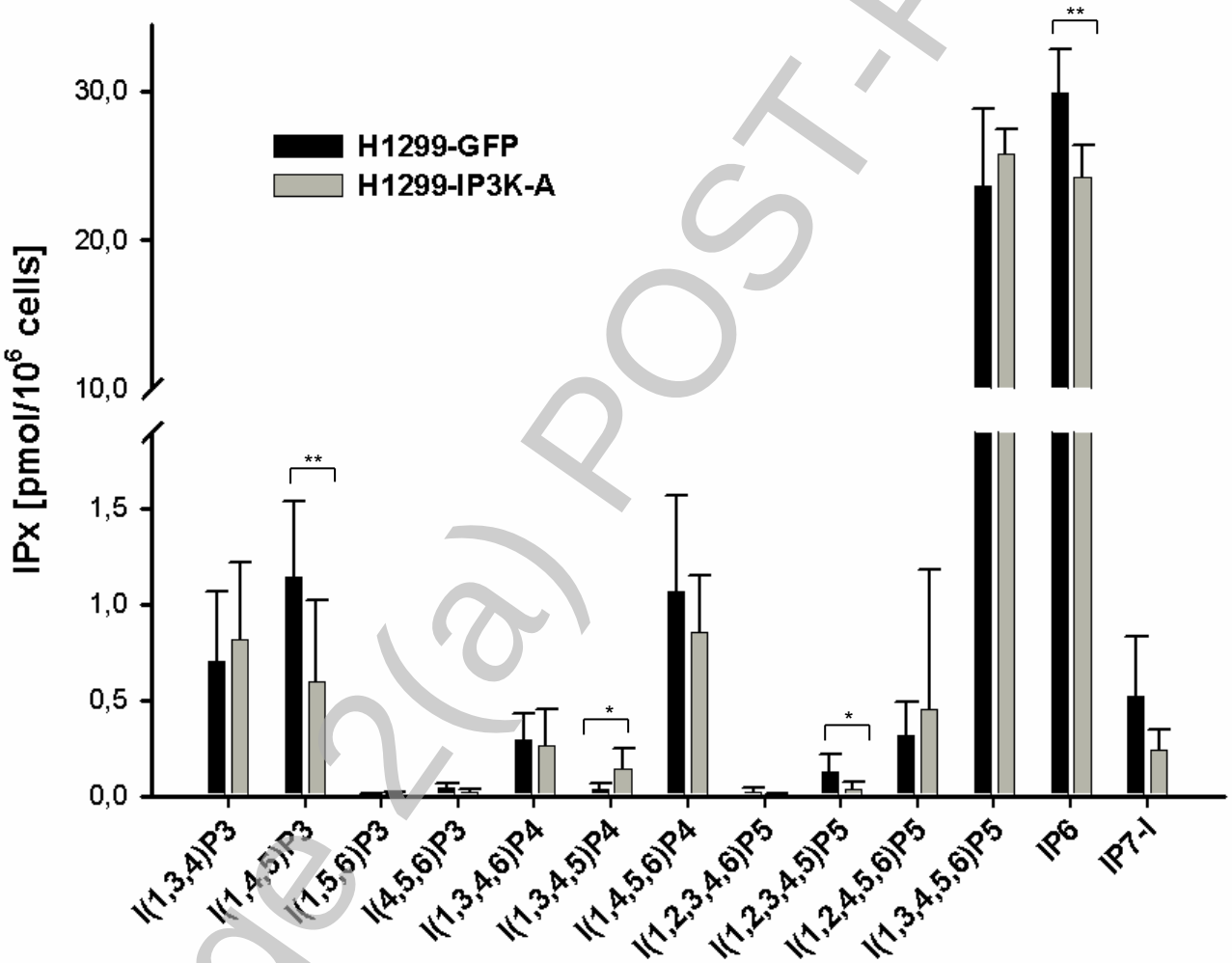

B

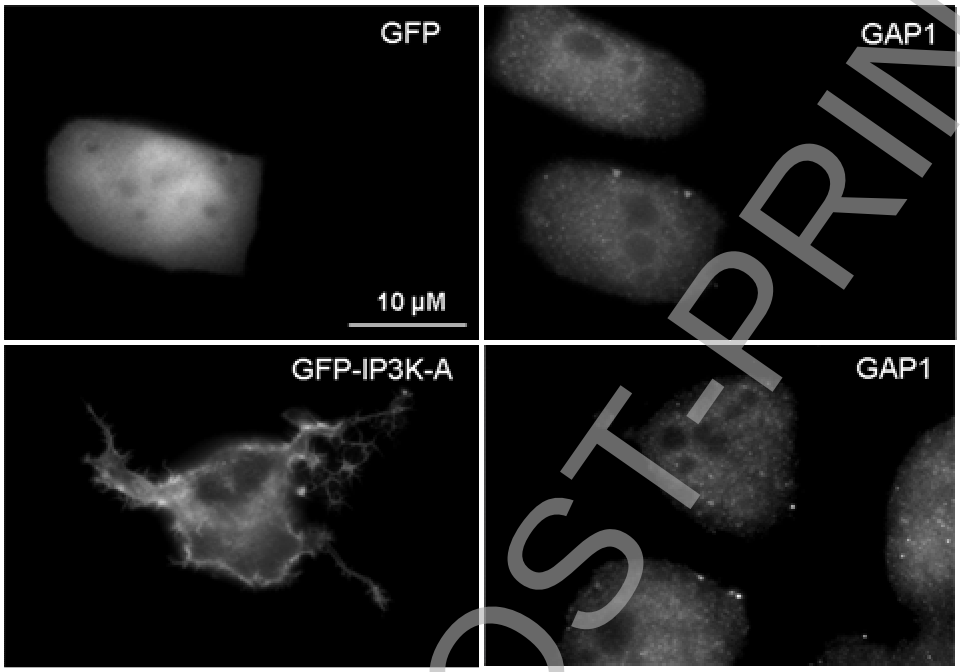

C

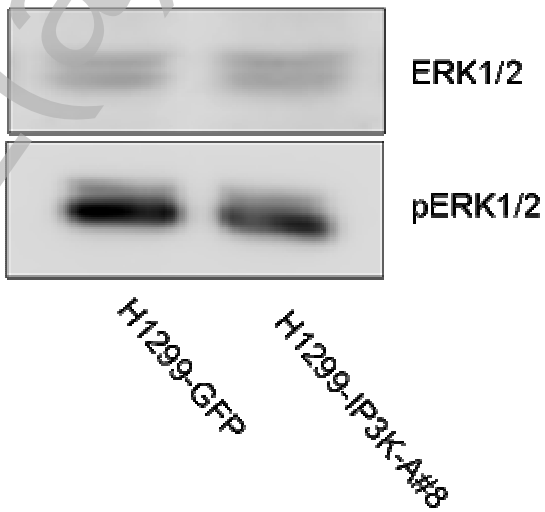

Figure 8

A

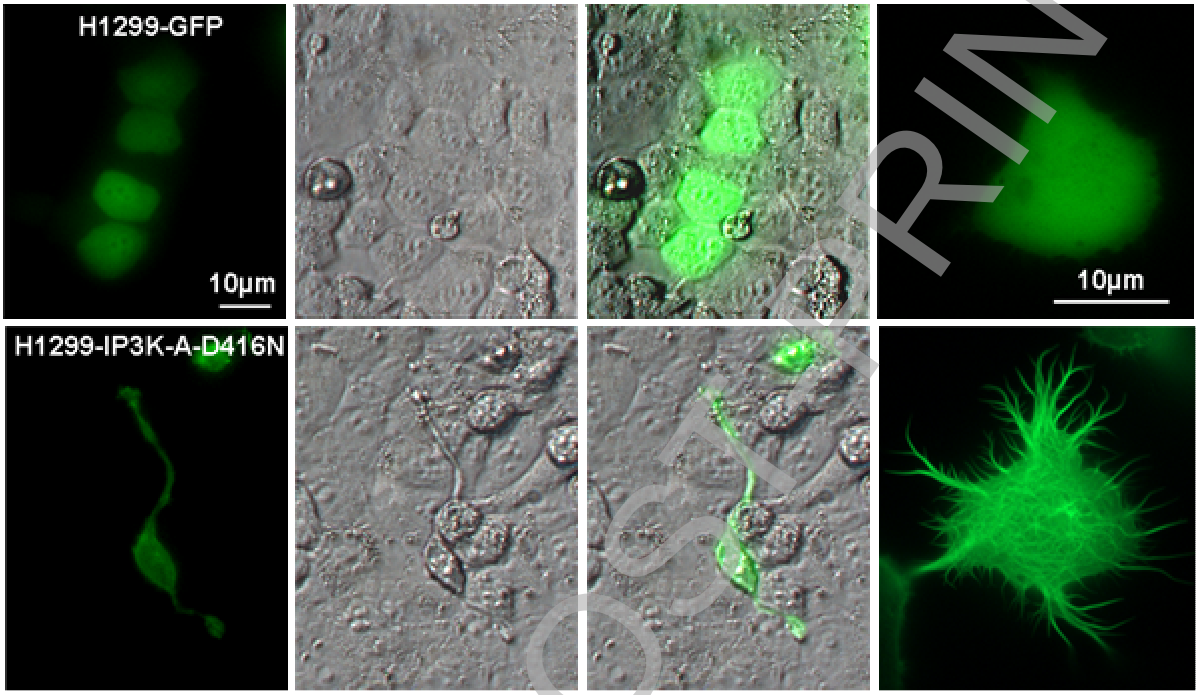

B

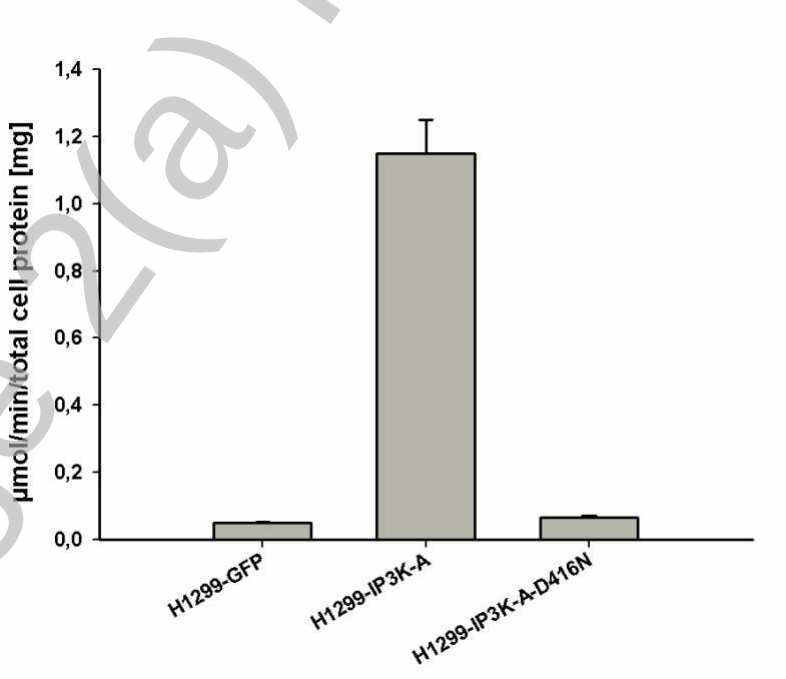

C

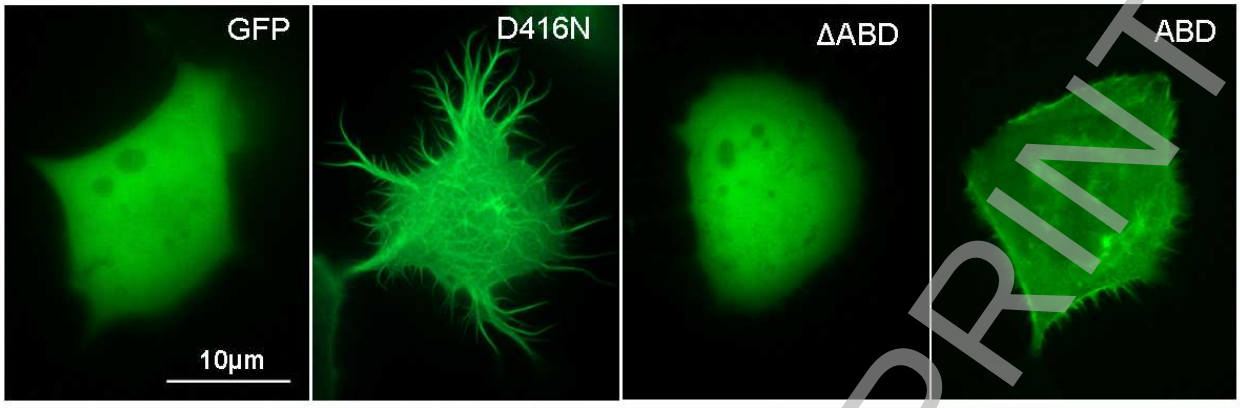

Morphology	H1299-GFP [%] cells	H1299-IP3K-A D416N [%] cells	H1299-IP3K-A ABD [%] cells	H1299-IP3K-A ΔABD [%] cells
(1) Many short filopodia	64 ± 4	10 ± 1.5	74 ± 6	78 ± 1
(2) Few filopodia	31 ± 8	7 ± 2	17 ± 3	15 ± 0.5
(3) Many branching filopodia	5 ± 0.5	37 ± 5	9 ± 3	7 ± 1
(4) Few branching long filopodia or lamellipodia	none	46 ± 3	none	none

D